Ultra-fast imaging with optical encoding and compressive sensing

Ultra-fast imaging with optical encoding and compressive sensing

Amir Matin, Bo Dai, Yu Huang, Xu Wang *Senior Member, IEEE*

***Abstract*—Serial time-encoded amplified microscopy (STEAM) is an emerging technology which enables an ultra-fast phenomena to be captured at Ghz scan rate. The trade-off between high imaging speed and high spatial resolution remains a problem where the maximum scan rate is limited by the sampling rate of the digitizer and the temporal dispersion in the fiber to avoid data blending. In this paper, we address these limitations using state-of-the-art optimization algorithms under compressive sensing framework and establish the data acquisition model based on our proposed experimental setup by considering the effect of individual optical components such as laser spectral profile, encoding mask patterns, dispersion of the fiber and optical noise in the system. We introduce two methods of alternating direction method of multipliers with total variation regularization (ADMM-TV) and discrete wavelet hard thresholding (DWT-Hrd) for STEAM based imaging systems. Our results demonstrate that a 10GHz scan rate can be achieved compared to the conventional 1GHz microscopy imaging system while maintaining high image reconstruction quality in terms of structural similarity index measurement (SSIM). It is shown that among the two proposed optimization algorithms, ADMM-TV outperforms DWT-Hrd by 20% in SSIM measurements. Finally, it is shown that having 70-80% light transmission through the mask reveals the optimum results in terms of reconstruction quality.**

***Index Terms*—fiber optics imaging, optical encoding, compressive sensing, optimization algorithms.**

I. Introduction

ULTRAFAST optical imaging has become one of the vital tools for capturing real-time and non-repeatable events such as blood cells screening, microfluidics, surface inspection and micro-PCB designs. Serial time-encoded amplified microscopy (STEAM) is an emerging ultrafast imaging technique which overcomes the fundamental trade-off between sensitivity and speed [1],[2]. Limitations on the STEAM technology, specially on the scan rate of the system, is restricted by the amount of dispersion and the spatial resolution of the setup. In the conventional STEAM systems, the spatially modulated optical pulses with a spectral bandwidth $\delta\lambda$ and repetition rate R, are stretched by dispersive fiber (with total dispersion D) in the time domain, causing a dramatic drop in the scan rate in order to avoid overlapping of adjacent signals (data mixing). This constraint can be written as

$$D \times \delta\lambda \leq \frac{1}{R} \tag{1}$$

The amount of dispersion D has a direct relation to the spatial resolution of the imaged section N and the sampling rate of digitizer S, that is

$$D = \frac{N}{S \times \delta\lambda} \tag{2}$$

Higher amount of dispersion is desirable as it enables a larger imaging area or higher spatial resolution in the imaging system. However, this will result in a lower scan rate due to the limitation defined by (1). Meanwhile, a higher scan rate is also crucial as it enables us to observe phenomena at more than 1GHz speed previously achieved in [1],[2]. This reveals the fundamental limitation of the conventional STEAM system where high spatial resolution and high imaging scan rates cannot be achieved simultaneously.

Another drawback of the conventional STEAM system becomes evident when longer scanning times result in a very large amount of data to be processed. Capturing of an ultra-fast phenomenon at the scan rate R (time resolution of $1/R$), spatial resolution N and duration L, requires the total amount of data of size $R \times N \times L$ to be processed in the system. Therefore, a processing unit with a maximum capacity G, imposes another constraint on the system, that is

$$G \geq R \times N \times L \tag{3}$$

Subsequently, the data processing capacity of conventional STEAM, limits the ability of the system to capture ultra-fast phenomenon with high spatial resolution at high scan rates and longer durations.

Studies to overcome these limitations have been carried out in [3], where the data compression has been achieved using differential detection run-length encoding techniques. In [4], the virtual time gating technique has been proposed where the signal is divided into multiple portions in a sequence of time slots and switched into parallel channels. Using virtual time gating can stretch the signal with a high dispersion for detection and potentially overcome the constraint in (1) however, the amount of dispersion is limited to avoid the heavy overlap between the signals. Virtual time gating will require multiple groups of detectors for signal detection which can be a costly solution. Furthermore, in the virtual time gating scheme, the signal is divided into different channels by using an optical coupler which can result in the reduction

Amir Matin and Xu Wang are with the Institute of Photonics and Quantum Sciences, School of Engineering and Physical Sciences, Heriot-Watt University, Edinburgh, EH14 4AS, U.K . (e-mail: x.wang@hw.ac.uk).

Bo Dai and Yu Huang are with the Engineering Research Center of Optical Instrument and System, the Ministry of Education, Shanghai Key Laboratory of Modern Optical System, University of Shanghai for Science and Technology, Shanghai, P.C. 200093, China.

This article has been accepted for publication in a future issue of this journal, but has not been fully edited. Content may change prior to final publication. Citation information: DOI 10.1109/JLT.2018.2880816, Journal of Lightwave Technology

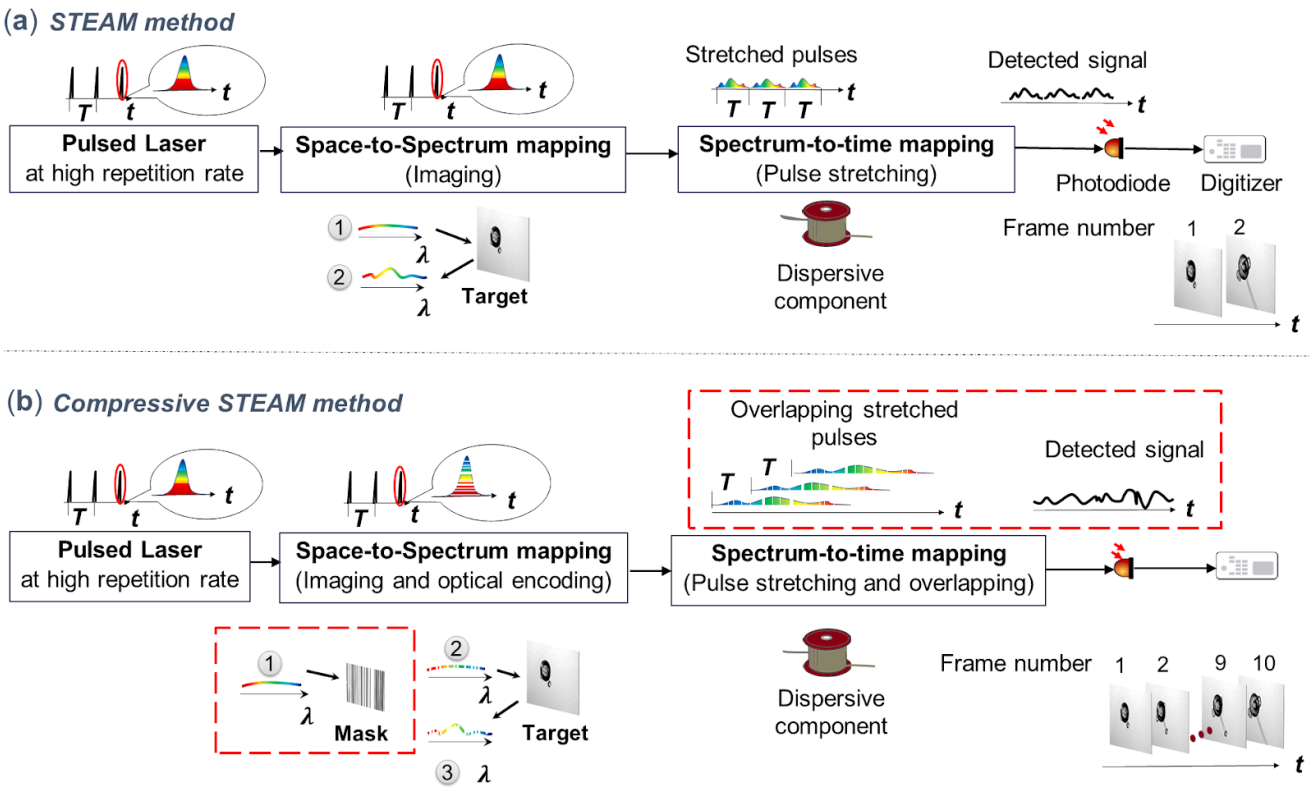

Fig. 1. Operation principles of (a) conventional STEAM system (b) proposed compressive imaging setup

of the signal power. In [5], an optical modulation scheme has been used to encode individual pulses, allowing partial overlap to improve the scan rate of the imaging system and using compressive sensing algorithm to reconstruct the image. In [6], sparse representations of signals are investigated in different domains and techniques such as dictionary learning and DCT transform have been proposed for reconstructing the original signals. Lastly, a new technique has been proposed in [7] which uses an imaging approach called asymmetric-detection time-stretch optical microscopy (ATOM) delivering fast label-free imaging. In this paper, we derive the mathematical data acquisition model of the ultrafast imaging system with compressive sensing and optical encoding while incorporating the physical parameters in the experimental setup including laser spectral profile, encoding mask patterns, fiber dispersion and noise in the mathematical model. We implement two methods of ADMM-TV (variational based) [8] and wavelet hard thresholding (sparsity-based) [9] to minimize the reconstruction error in an iterative fashion and achieve low error data recovery by considering our prior knowledge about the data in the optimization algorithms. These methods have been previously implemented for various types of applications such as video compressive sensing [10], [11] for motion detection and compensation [12]-[15], multiscale photography [16] and bio-imaging [17] and have shown superior performances compared to the other optimization methods however, they have never been implemented for STEAM imaging systems.

II. Experimental Setup of Imaging System

Fig.1(a) shows the operation principle of the STEAM imaging system formed by spatial encoding, pulse stretching and single-pixel detection stages. In the spatial encoding stage, the spectrum of the ultra-short optical pulses produced at a high repetition rate (shown as 1 in Fig. 1(a)) is spatially dispersed and modulated by a target resulting in space-to-spectrum mapping. In the next step, the spatial information of the target is mapped onto the spectrum of the optical signal which is shown as 2 in Fig. 1(a). This process is known as spectral-amplitude-encoding and is widely used in optical communications for optical code division multiple access (OCDMA) [18]. In the second stage, the spectrally modulated pulses are further stretched through a dispersive component resulting in spectrum-to-time mapping which enables the signal to be detected by a fast single-pixel photodetector. Finally, these detected signals are reconstructed back to their original form by converting the array of 1-D signals into 2-D frames through a processing unit.

Fig. 1(b) shows the operation principles of the proposed compressive imaging scheme. In the spatial encoding stage, the optical spectrum of an ultra-short optical pulse (shown as 1) is first encoded by a binary mask pattern (shown as 2) before the space-to-time mapping (shown as 3). In the second stage, overcoming the scan rate limitation of STEAM setup (R in (1)) is tackled by further stretching the signals and allowing consecutive scans to overlap through a dispersive component resulting in much higher imaging rate without compromising the spatial resolution of the imaging system. In the proposed scheme, the received data is heavily compressed and the total amount to be processed remains the same vector size from those obtained in conventional STEAM setup, allowing the system to record a longer duration of an ultra-

This article has been accepted for publication in a future issue of this journal, but has not been fully edited. Content may change prior to final publication. Citation information: DOI 10.1109/JLT.2018.2880816, Journal of Lightwave Technology

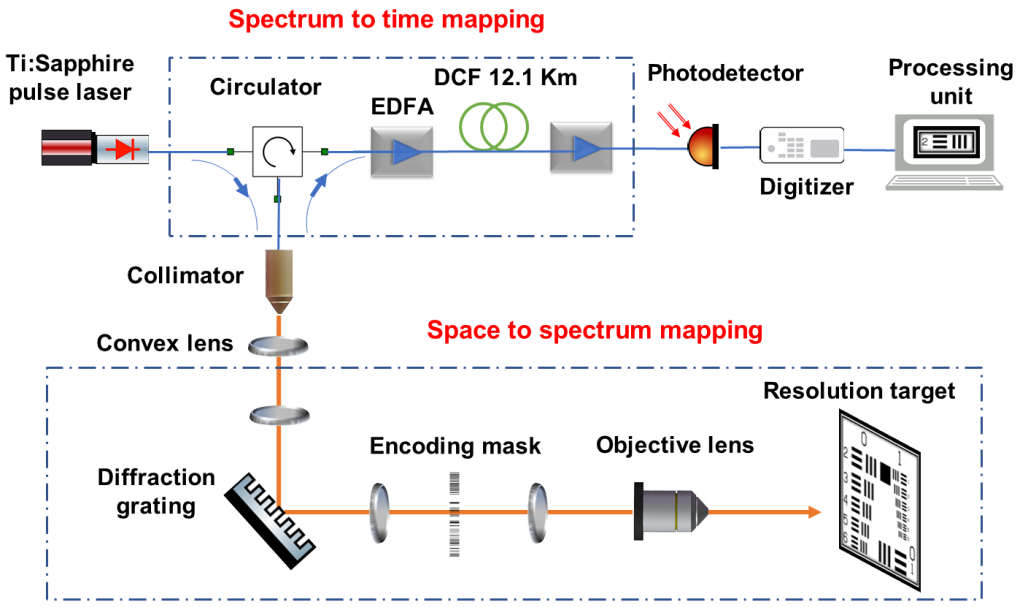

Fig. 2. Experimental setup of the proposed scheme

fast event. As the detected signals are overlapped pulses, an inverse mathematical model is required to reconstruct the mixed signals using optimization algorithms. Fig. 2 shows the experimental setup of the proposed scheme where optical pulses with a central wavelength of 1550nm and bandwidth of 40nm generated from the 1GHz Ti:Sapphire femtosecond laser are directed towards a diffraction grating. The spectrum of the diffracted signal is then encoded by a binary mask pattern and focused on a time-varying target. This process is the space to spectrum mapping depicted in Fig. 1(b). The reflected light from the target is then amplified by an erbium-doped fiber amplifier (EDFA) and fed into a dispersive fiber (DCF) which stretches the pulses in the time domain (shown as spectrum-to-time mapping in Fig. 1). Individual pulses carry spatial information about the dynamic scene which are generated at the repetition rate of the laser. The dispersion value of the DCF is chosen in a way that the stretched pulses in the time domain have a significant overlap between the adjacent pulses. This is breaking the limitation determined in (1), by allowing $D \times \delta\lambda \gg 1/R$. As a result, achieving much higher scan rate is facilitated in the proposed scheme. Using a random mask per scan enhances the performance of the recovery algorithms by minimizing the correlation between the adjacent signals. Applying a fully random mask per scan is one of the main challenges imposed on the compressive STEAM imaging systems where the maximum encoding rate of 300KHz is achievable in digital spatial light modulators however, this type of encoding can be beneficial on the targets with slower flow rates where by applying the compression, a longer period of the phenomenon can be recorded. Imaging of the resolution target is an important step as it defines crucial factors of the physical setup such as the spatial resolution of the imaging system, the spectral shape of the source and the amount of accumulated (Gaussian) noise in the system. This process can be thought as a calibration stage where the original spatial information of the target scene is known and the output read-out from the photodetector reveals the spectral profile of the laser, defining the critical boundaries of spatial resolution of the system and the amount of present noise.

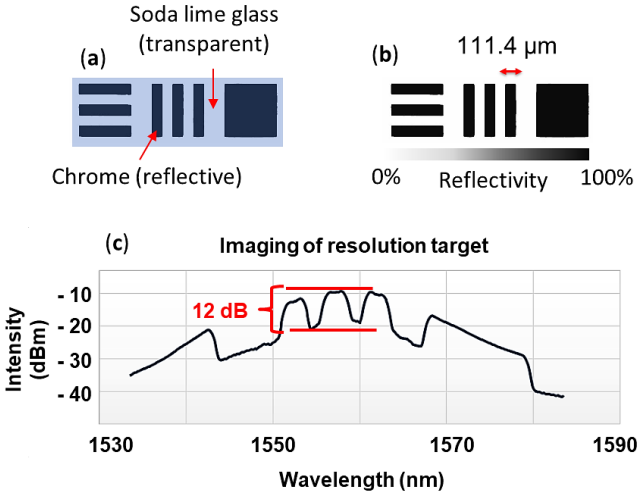

Fig. 3. Imaging of the resolution target
(a) The bright-field microscopic image
(b) The image obtained from proposed setup
(c) The measured spectrum of the first scan line

The resolution of our imaging setup is measured by imaging the patterns of standard USAF-1951 resolution test target depicted in Fig. 3. In the experiment, the DCF has the length of 12.1 km and the chromatic dispersion is 1573 ps/nm. Each chrome line has a width of 111.4 μm and the conversion factor between space and wavelength is 2.77 μm/nm. Fig. 3(a) shows the image of the target captured by a conventional microscope and Fig. 3(b) is the captured image with dimensions of 100 ×

This article has been accepted for publication in a future issue of this journal, but has not been fully edited. Content may change prior to final publication. Citation information: DOI 10.1109/JLT.2018.2880816, Journal of Lightwave Technology

250 pixels in our system. Fig. 3(c) shows a 12 dB difference between the transmissive and reflective sections of the target defining the minimum dynamic range in the system. The detected signal has a high Signal-to-noise ratio (SNR), however, denoising step is still required in the reconstruction algorithm due to the presence of thermal and shot noise in the system. The setup of the imaging system is modified as depicted in Fig. 4 for imaging of the human blood flowing in a microfluidic chip. After the light diffraction, beam size adjustment and spectrum modulation, the light is then coupled into a pair of objective lenses, which are used to capture the microscopic image of blood flow in the microfluidic chip channel. The diffraction grating has the groove density of 600 lines/mm with the diffraction angle of 30 degrees and an input beam waist of 7.2 mm. The spectral and the spatial resolution of the setup are 0.3 nm and 0.82 μm respectively with the space-to-wavelength conversion factor of 2.74 μm/nm. Objective lenses for cell detection have a numerical aperture of 0.65 and focal length of 4 mm. Microcells contained in a chemical fluid are injected into a microfluidic chip with dimensions of 50 × 30 μm and the flow rate of 2 m/s. In the wavelength-to-time mapping stage, the optical power before and after the amplification is 27 and 632 μW respectively.

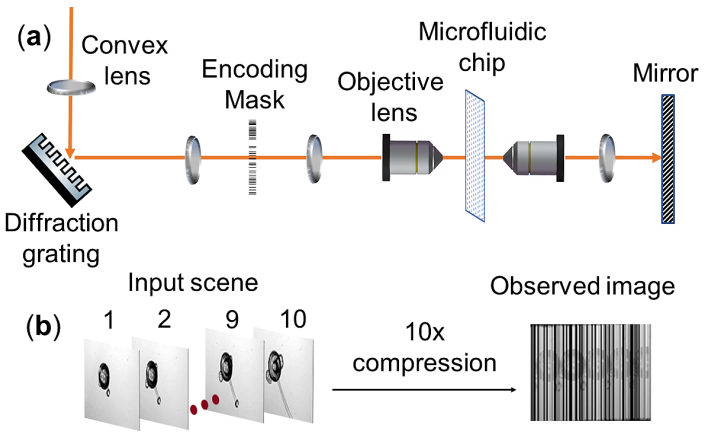

Fig. 4. (a) Modified setup for cell detection (b) Observed compressed data

Obtained results from the modified setup are depicted in Fig. 4(b) exhibiting the 2-D transformation of the detected signal from the single-pixel photodetector. This data is formed by optically encoding the spectrally modulated pulses and overlapping 10 consecutive stretched pulses in the dispersive component.

III. Modelling of Data Acquisition and Reconstruction Process

Here, we establish the data acquisition model of the proposed scheme by considering the properties of the optical components in the system helps us to optimize the parameters of the reconstruction algorithm to achieve the minimum data loss. The mathematical expression of the data acquisition model in the system is formulated as

$$y = HALx + n \tag{4}$$

where $y \in \mathbb{R}^{M+(N-1)sM\times 1}$ is the captured data, s is the ratio of the pulse period $(1/R)$ to the width of the stretched pulse $(D \times \delta\lambda)$ referred to as the shift ratio where $0 \leq s \leq 1$, $H \in \mathbb{R}^{M+(N-1)sM\times MN}$ is the linear operation of shifting and overlapping, $A \in \mathbb{R}^{MN\times MN}$ is the binary mask as a diagonal matrix, $L \in \mathbb{R}^{MN\times MN}$ is the laser spectral profile as a diagonal matrix, $x \in \mathbb{R}^{MN\times 1}$ is the original data and n is the noise in the system. y represents the summation of the individually encoded and temporally overlapped scan lines containing multiplexed information about the dynamic scene. M and N are the numbers of sampled points in a single scan line and the total number of scans respectively. DCF stretches the spectrally modulated signals (carrying the spatial information of the image) in the time domain where a high dispersion value of DCF allows the adjacent pulses to partially overlapped and form a heavily compressed observation of the fast dynamic scene. This key operation is noted as H in the acquisition model shown in (4). H is built upon N identity matrices with dimension of $I \in R^{(M\times M)}$ where the starting position of individual I_h $(1 \leq h \leq N)$ in H is calculated based on its index value. Assuming i, j are the starting position of I_h in H, they can be calculated as

$$i = (h-1)M + 1 \quad and \quad j = s(h-1)M + 1 \tag{5}$$

where the rest of the elements in H are set to zero. The matrix representation of H is depicted in Fig. (5)

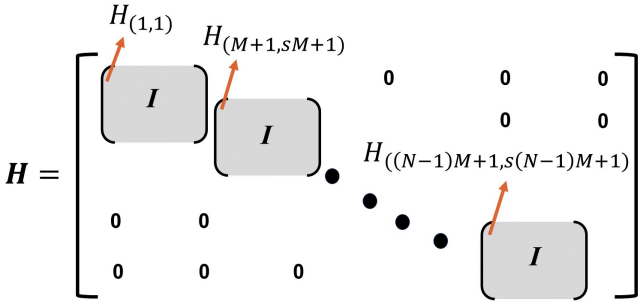

Fig. 5. Representation of the matrix H

The compression ratio between the original and overlapped detected signal is controlled by the shift ratio(s) used in-between the adjacent pulses which is determined as

$$\text{Compression ratio} = \frac{N}{1 + (N-1) \times s} \tag{6}$$

Estimating x from y in (4) is known as an *ill-posed* linear inverse problem (LIP) [19]. Consequently, this problem requires additional regularization (or prior information) in order to reduce uncertainties and improve estimation performance. Therefore, state-of-the-art convex optimization algorithms for solving such problems can be used. While the sensing matrix noted as HAL in (4) enables a high optical compression on the data, it does not satisfy the Restricted Isometry Property (RIP) [20] used in compressive sensing framework therefore, the reconstruction is known as a lossy recovery. As the captured data from our system are representing the spatial information of a natural scene, we can assume that they can also be

This article has been accepted for publication in a future issue of this journal, but has not been fully edited. Content may change prior to final publication. Citation information: DOI 10.1109/JLT.2018.2880816, Journal of Lightwave Technology

represented in a sparse fashion in another domain. One of these sparse domains is the discrete wavelet transform (DWT) [21], [22] which has attracted considerable experimental and theoretical attention due to the fast and optimized transform calculations and flexibility to be modified and used for different types of applications in various areas such as compressive sensing, hyper-spectral and medical imaging. Second proposed approach is to solve the minimization problem by iteratively calculating the total variation (TV) [23]-[25] of the signal and minimizing the energy function. This approach takes advantage of signal representation in the gradient domain and calculates the ℓ_1 norm of the gradient to minimize the cost function.

A. Sparse Regularization

Sparsity-based methods aim to recover the signals by finding an appropriate domain for the data where they can be transformed and represented in a sparse fashion. In the proposed model, sparse set of coefficients $\hat{a}$ in the domain Ψ are given by

$$\widehat{a} = \underset{a}{argmin}\, \frac{1}{2}||HAL(\Psi a)) - y||_2^2 + \lambda||a||_1 \qquad (7)$$

where λ is the prior weight which is adapted to the noise level in the signal. Combining the shifting and overlapping operator H, encoding operator A and the spectral profile of the laser L, results in a new operator $\boldsymbol{\phi}$ which represents the joint linear operation where $\boldsymbol{\phi} = HAL$. We use the forward-backward splitting method [26] to solve (7) which is a non-smooth optimization problem. In (8), we apply the gradient descent step in the spatial domain and implement hard thresholding schemes for the calculated coefficients in the wavelet domain, that is

$$x^{k+1} = Thr_{\lambda}^{\psi}(x^k - \tau(\phi^T(\phi(x^k) - y)) \qquad (8)$$

where τ is the gradient step constant and ϕ^T is the transpose of the linear operator ϕ. To solve (8), an iterative solution is shown in algorithm 1. The stopping criteria for this algorithm is defined by the convergence of the Frobenius norm of the energy function which is defined as

$$E^{k+1} = \frac{1}{2}||\phi(\hat{x}) - y||_F^2 \qquad (9)$$

B. Variational Regularization

Second method to solve (4) is to minimize the energy function in spatial domain and using the total variation as the regularizer which is given by

$$\widehat{\boldsymbol{x}} = \underset{x}{argmin}\, \frac{1}{2}||y - \phi(x)||_2^2 + \lambda||Dx||_1 \qquad (10)$$

where D computes the gradient of x in vector dimensions.

There are several methods to solve (10) however we propose to use ADMM method which applies variable splitting to (10) and solves the produced Lagrange equations by introducing a new regularizer ρ_k into the equation. ADMM splits Lagrange into two separate equations and solves them cyclically. We also introduce a new variable ρ_{tv} as a variable smoothing parameter which varies based on the calculated residual values at each iteration shown as steps 11-14 in algorithm 2 where

$$\text{Res}_{\text{ total}} \overset{\text{def}}{=} ||x^{k+1} - x^k||_2 + ||v^{k+1} - v^k||_2 + ||u^{k+1} - u^k||_2 \qquad (11)$$

The adaptive update scheme is inspired from [27], which was originally used to accelerate ADMM algorithms for convex problems. It is different from the residual balancing technique commonly used in ADMM, e.g., [8], as $\text{Res}_{\text{total}}$ sums of all primal and dual residues.

Algorithm 1: Estimation based on wavelet translation invariant hard thresholding method

Input: $y \in \mathbb{R}^{\,M+(N-1)sM\times 1}$: Observed
Output: $\hat{x} \in \mathbb{R}^{MN\times 1}$: reconstructed data
Operation ψ : wavelet transform
Operation ψ^{-1} : inverse wavelet transform
Initialize $\hat{x} = \phi^T(y)$, v, u as zero matrix
Initialize $\tau \geq 1$, $1 > \lambda \geq 0$, tolerance $= 10^{-4}$
(I)**repeat**
  $u = \hat{x} - \tau\phi^T(\phi(\hat{x}) - y)$
  where ϕ is the joint operation of HAL
  $v =$ hard thresholding$(\psi(u), \lambda)$
  $\hat{x} = \psi^{-1}(v)$
  $E^{k+1} = \frac{1}{2}||\phi(\hat{x}) - y||_F$
(I) **until** $E^{k+1} - E^k \leq$ tolerance
return $\hat{x}^{(k)}$

Algorithm 2: Estimation based on ADMM weighted TV and residual based updating parameters

Input: $y \in \mathbb{R}^{\,M+(N-1)sM\times 1}$: Observed
Output: $\hat{x} \in \mathbb{R}^{MN\times 1}$: reconstructed data
Initialize $\hat{x}$, $\hat{v}$, u as zero matrix, $\mu > 0$, residuals $\text{Res}_{\text{ x}}$, $\text{Res}_{\text{ v}}$, $\text{Res}_{\text{ u}}$, $\text{Res}_{\text{ total}}$, $\rho_{tv\ (max)}$ as $\sqrt{\frac{\lambda}{\rho_k}}$ and $\rho_{tv\ (min)}$ as $\frac{\rho_{tv\ (max)}}{10}$, $\gamma > 1$
(I) **while** (tolerance $\leq \text{Res}_{\text{ total}}$)
  (II) **while** $\rho_{tv}\ != \ \rho_{tv\ min}$
    $v^{(k-1)} = \hat{v}$, $u^{(k-1)} = u^k$
    $\tilde{x} = v^{(k-1)} - u^{(k-1)}$
    $\hat{x} = \underset{\hat{x}}{\text{argmin}}\, ||\phi\hat{x} - y||_2^2 + (\rho_k/2)||\hat{x} - \tilde{x}||_2^2$
    $\tilde{v} = \hat{x} + u^{(k-1)}$
    $\hat{v} = TV\ (\tilde{v}, \rho_{tv\ (\text{updated})})$
  Update Lagrange multiplier
    $u^k = u^{(k-1)} + (\hat{x} - \hat{v})$
  Update $\text{Res}_{total} = \text{Res}_x + \text{Res}_v + \text{Res}_u$
    if $\text{Res}_{total}^k \leq \text{Res}_{total}^{k-1}$
      keep current ρ_{tv} and ρ_k
    else
      $\rho_{tv_{k+1}} = \frac{\rho_{tv_k}}{2}$, $\rho_{k+1} = \gamma\rho_k$
  (II) **end**
  $k = k + 1$
(I) **end**
return $\hat{x}^{(k)}$

This article has been accepted for publication in a future issue of this journal, but has not been fully edited. Content may change prior to final publication. Citation information: DOI 10.1109/JLT.2018.2880816, Journal of Lightwave Technology

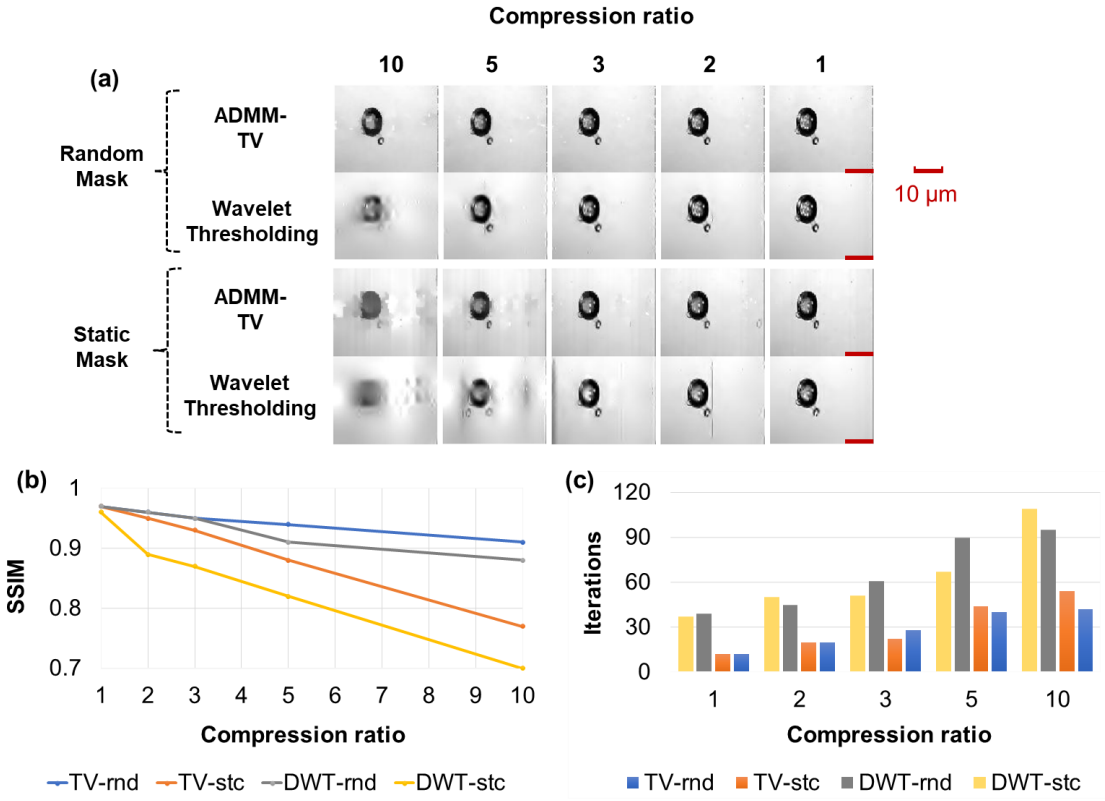

Fig. 6. Reconstruction of detected blood cell samples under various compression ratios

The proposed methods of ADMM-TV and DWT-Hrd can be adapted for the cases of 2D imaging systems such as [1], [2] where 2D spatial disperser and a 2D encoding mask can facilitate such imaging setups. Assuming the original frames forming the data cube $x_{cube} \in \mathbb{R}^{M\times N\times F}$ where M, N, and F are the number of rows, columns and total frames respectively. The mathematical representation of the forward model for this setup will be the same as (4) where y $\in \mathbb{R}^{MN+(F-1)sMN\times 1}$ is the captured data, H $\in \mathbb{R}^{MN+(F-1)sMN\times MNF}$ is the linear operator of shifting and overlapping, A $\in \mathbb{R}^{MNF\times MNF}$ is the encoding frames as a diagonal matrix, L $\in \mathbb{R}^{MNF\times MNF}$ is the laser spectral profile as a diagonal matrix, x $\in \mathbb{R}^{MNF\times 1}$ is the vectorised original frames and n is the additive zero mean Gaussian noise. ADMM-TV and DWT algorithms can reconstruct the data in the aforementioned dimensions and reshape the recovered data back into their 3D original format.

IV. Results and Discussion

Fig. 6(a) shows the reconstructed frames from the reaction of a blood cell to an external injected chemical substance. Comparison between the two methods (depicted in Fig. 6(b)) demonstrates that TV-based algorithms (TV-rnd and TV-stc) outperform hard thresholding wavelet-based methods in both random and static mask cases (DWT H-thr-rnd and DWT H-thr-stc) with an average higher structural similarity of 20%. The data recovery at 100% transmission (no encoding) also shows the superior performance of ADMM-TV over DWT algorithm. This is mainly due to the fact that TV recognizes the edge features in the images and preserves them from hard smoothing in the algorithm which can result in spatial information to merge and therefore losing critical information such as clear feature boundaries and intensity amplitudes per pixels. Depicted results for the statically encoded scene are realized through the experimental measurements. Those with the randomly encoded masks have been obtained through our simulations where the scene is first realized through the conventional STEAM setup. The random encoding, compression and the noise are then applied to the data prior to their reconstruction. Compression plays a crucial part in the quality of the reconstructed frames where higher compression ratios introduce larger amounts of reconstruction artefacts due to the cross-talk between the heavily overlapped rows. Solid lines in Fig. 6(b) show the SSIM values against the compression ratio when using a static mask as an encoder. The same reconstruction process is applied on randomly encoded scan lines where the individual pulses benefit from distinct masking patterns. Reconstructed images from randomly encoded scans show higher visual similarity (predominantly after 5 times compression ratio) to the original data as depicted in Fig. 6(a,b) due to the minimized correlation between overlapped pulses. The required number of iterations for the convergence of the presented algorithms are depicted in Fig. 6(c). TV based algorithms require almost half the number of iterations to those in DWT methods which can make a significant difference when dealing with larger amounts of data. The recorded time for each iteration is $\approx$ 0.1(sec). Static coding mask applies the same pattern on individual pulses which

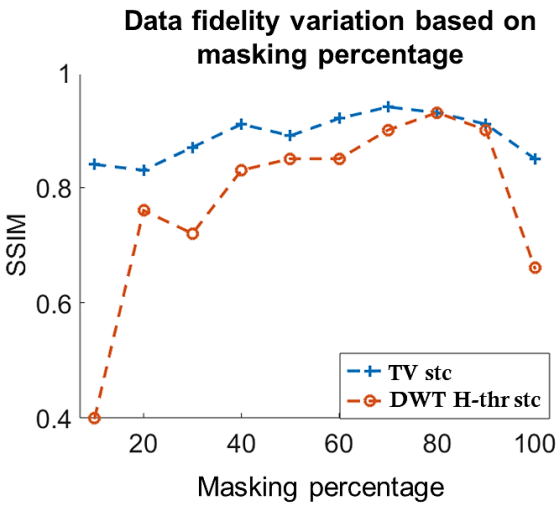

Fig. 7. Optimal mask estimation

is not ideal as having the same code for all the scan lines introduces correlation errors in the reconstruction algorithm hence various masking percentages can have a large impact on minimizing the reconstruction error. By varying the masking percentage (the ratio between 0s and the total number of pixels in the mask), an optimal masking amount is defined. Depicted results in Fig. 7 are obtained through the simulations where at each masking percentage, 10 randomly generated patterns are implemented and the calculated SSIM results have been averaged. From Fig. 7, it is shown that the peak SSIM value for ADMM-TV algorithm is achieved at 70% light transmission however the DWT algorithm performs better at 80% transmission hence the optimal masking percentage depends on the type of the optimization algorithm.

V. Conclusion

In this paper, the main limitations of the conventional STEAM imaging setup have been tackled using a new proposed scheme where by applying optical encoding and scan overlapping, a laser with a higher repetition rate (up to 10GHz) can be implemented while keeping the digitizer at the initial sampling rate. Mathematical data acquisition model is derived based on the properties of the proposed compressive STEAM imaging setup where the response from individual system components have been profiled and implemented as prior assumptions for the reconstruction algorithms of the received signals. Observed data were reconstructed under CS framework using two methods of ADMM-TV and DWT-Hrd, facilitating scan rates of 10GHz while keeping a high data fidelity and achieving 0.7 SSIM for **10 times** compression ratio. Moreover, proposed scheme benefits from having no mechanical moving parts since the spatial encoding is applied using a static pre-printed binary mask. The encoding stage is further investigated by applying two variations of static and random patters where the superior performance of ADMM-TV has been demonstrated for both patterns reaching an average higher SSIM of 20% due to the advanced edge preservation properties in this algorithm. Finally, we have investigated the optimal masking percentage and revealed that by having 70 to 80% light transmission through the mask, optimal reconstruction can be achieved. Considering the fact that using the proposed scheme can potentially enhance the performance of the conventional STEAM system while requiring minimal changes to the typical setup, we hope and anticipate that this may prove to be of some interest and usefulness to others employing the similar approaches for the study of other high-throughput imaging systems.

Acknowledgment

We would like to thank Scottish Universities Physics Alliance (SUPA) for their contributions and financial support throughout this work.We are also grateful to Dr A. Belyaev for his insightful contributions and also Prof. Guodong Sui and Dr. Lulu Zheng of Fudan university for providing blood cell samples.

References

[1] K. Goda, K. K. Tsia, and B. Jalali, Serial time-encoded amplified imaging for real-time observation of fast dynamic phenomena, Nature, vol. 458, pp. 11451149, Apr. 2009

[2] K. K. Tsia, K. Goda, D. Capewell, and B. Jalali, Performance of serial time-encoded amplified microscope, Opt. Express, vol. 18, no. 10, pp.10016 10028, Apr. 2010.

[3] B. Dai, S. Yin, Z. Gao, K. Wang, D.Zhang, S.Zhuang, X.Wang, "Data Compression for Time-Stretch Imaging Based on Differential Detection and Run-Length Encoding," in Journal of Lightwave Technology, vol.35, no.23, pp.5098-5104, Dec.1,12017.

[4] Y. Han and B. Jalali, "Continuous-time time-stretched analog-to-digital converter array implemented using virtual time gating," in IEEE Transactions on Circuits and Systems I: Regular Papers, vol. 52, no. 8, pp. 1502-1507, Aug. 2005.

[5] C. Lei, Y. Wu, A.C. Sankaranarayanan, S. Chang, B. Guo, N. Sasaki, H. Kobayashi, C. Sun, Y. Ozeki, K. Goda, "GHz Optical Time-Stretch Microscopy by Compressive Sensing," in IEEE Photonics Journal, vol. 9, no. 2, pp. 1-8, April 2017.

[6] Qiang Guo, Hongwei Chen, Zhiliang Weng, Minghua Chen, Sigang Yang, and Shizhong Xie, "Fast time-lens-based line-scan single-pixel camera with multi-wavelength source," Biomed. Opt. Express 6, 3610-3617 (2015)

[7] T. W. Wong, Terence K. S. Lau, Andy Tang, Matthew Yuk Heng Ho, Kenneth K.Y. Wong, Kenneth H. C. Shum, Anderson Tsia, Kevin. (2014). Asymmetric-detection time-stretch optical microscopy (ATOM) for high-contrast and high-speed microfluidic cellular imaging. Progress in Biomedical Optics and Imaging.

[8] S. H. Chan and O. A. Elgendy, "Plug-and-Play ADMM for Image Restoration: Fixed-Point Convergence and Applications," in IEEE Transactions on Computational Imaging, vol. 3, no. 1, pp. 84-98, March 2017

[9] I. W. Selesnick, R. G. Baraniuk and N. C. Kingsbury, "The dual-tree complex wavelet transform," in IEEE Signal Processing Magazine, vol. 22, no. 6, pp. 123-151, Nov. 2005

[10] E. J. Candes, J. Romberg and T. Tao, "Robust uncertainty principles: exact signal reconstruction from highly incomplete frequency information," in IEEE Transactions on Information Theory, vol. 52, no. 2, pp. 489-509, Feb. 2006.

[11] A. C. Sankaranarayanan, C. Studer, and R. G. Baraniuk, CS-MUVI: Video compressive sensing for spatial-multiplexing cameras, in Proc. IEEE Int. Conf. Comput. Photogr., Apr. 2012, pp. 110.

[12] R. Koller, L. Schmid, N. Matsuda, T. Niederberger, L. Spinoulas, O. Cossairt, G. Schuster, and A. Katsaggelos, "High spatio-temporal resolution video with compressed sensing," Opt. Express 23, 15992-16007, 2015

[13] J. Holloway, A. Veeraraghavan, and S. Tambe. Flutter shutter video camera for compressive sensing of videos. In ICCP, 2012

[14] D. Reddy, A. Veeraraghavan, and R. Chellappa. P2C2: Programmable pixel compressive camera for high speed imaging. CVPR, 2011

[15] A. Veeraraghavan, and R. Raskar. Coded strobing photography: Compressive sensing of high speed periodic videos. IEEE T-PAMI, 2011

[16] D.J. Brady, M.E. Gehm, R.A. Stack, D.L. Marks, D.S. Kittle, D.R. Golish, E.M. Vera, and S.D. Feller. Multiscale gigapixel photography. Nature, 486(7403):386389, 2012
[17] Y. Le Montagner, E. Angelini and J. C. Olivo-Marin, "Video reconstruction using compressed sensing measurements and 3d total variation regularization for bio-imaging applications," 2012 19th IEEE International Conference on Image Processing, Orlando, FL, 2012, pp. 917-920.
[18] Xu Wang and Naoya Wada, "Spectral phase encoding of ultra-short optical pulse in time domain for OCDMA application," Opt. Express 15, 7319-7326 (2007)
[19] E. J. Candes and M. B. Wakin, "An Introduction To Compressive Sampling," in IEEE Signal Processing Magazine, vol. 25, no. 2, pp. 21-30, March 2008.
[20] Emmanuel J. Candès, The restricted isometry property and its implications for compressed sensing, Comptes Rendus Mathematique, Volume 346, Issues 9–10, 2008, Pages 589-592
[21] I. W. Selesnick. Hilbert transform pairs of wavelet bases. IEEE Signal Processing Letters, 8(6):170-173, June 2001
[22] N. G. Kingsbury. Complex wavelets for shift invariant analysis and filtering of signals. Applied and Computational Harmonic Analysis, 10(3):234-253, May 2002
[23] L. Rudin, S. Osher, and E. Fatemi. Nonlinear total variation based noise removal algorithms. Physica D, 60:259268, 1992
[24] A. Chambolle. An algorithm for total variation minimization and applications. J. of Math. Imaging and Vision, 20:8997, 2004
[25] A. Chambolle. Total variation minimization and a class of binary MRF models. In Energy Minimization Methods in Computer Vision and Pattern Recognition, volume 3757 of Lecture Notes in Computer Sciences, pages 136152. Springer, 2005
[26] Hugo Raguet, Jalal M. Fadili, Gabriel Peyr. A Generalized Forward-Backward Splitting. SIAM Journal on Imaging Sciences, Society for Industrial and Applied Mathematics, 2013, 6 (13), pp.1199-1226.
[27] T. Goldstein, B. O' Donoghue, S. Setzer, and R. Baraniuk, "Fast alternating direction optimization methods," Tech. Rep., UCLA, 2012, Available online: ftp://ftp.math.ucla.edu/pub/camreport/cam12-35.pdf

Amir Matin received his degree in electronics and software engineering from Heriot Watt University, Edinburgh, UK, in 2013. He has worked as a software engineer in multiple international companies based in the UK from 2013 to 2016. Currently he is pursuing his Ph.D. in digital signal processing and fast optical imaging systems. His research interest includes image, video and signal processing, optical encoding, compressive sensing and fast optimization algorithms.

Bo Dai received the B. Eng. (First-class Honour) degree in the College of Science and Engineering, City University of Hong Kong in 2009, and Ph.D. degree in the Institute of Photonics and Quantum Sciences, Heriot-Watt University, UK, in 2013. From 2011 to 2012, he was with the National Institute of Information and Communications Technology (NICT), Japan, as an Internship Research Fellow. He is currently an associate professor in the University of Shanghai for Science and Technology. His research interests include optical imaging, optical communication and optical signal processing.

Yu Huang received the B.S. degree in information engineering from Xi'an Jiaotong University, Xi'an, China, in 2016. He is currently working toward the master's degree in signal and information processing with the University of Shanghai for Science and Technology, Shanghai, China. His research interests include optical secure communication and fiber optics.

Xu Wang received Ph.D. degree in electronic engineering from the Chinese University of Hong Kong (CUHK). He has been working in the National Key Laboratory of Fiber Optic Broad-band Transmission and Communication Networks of UESTC, China (1992 1997), the Department of Electronic Engineering of CUHK (2001 2002), Department of Electronic and Information Systems of Osaka University, Osaka, Japan (2002 2004), Photonic Network Group of National Institute of Communication and Information Technology (NICT), Tokyo, Japan (2004 2007). He is now an Associate Professor in the Institute of Photonics and Quantum Sciences, Heriot Watt University, UK. His research interests include ultra-fast imaging, signal processing, and optical communication systems. He has over 200 journal/conference publications and held 8 granted patents.